L-BAND TONE-CODE-DATA TRANSPONDER CALIBRATION

January 6, 1977

Prepared for
NATIONAL AERONAUTICS AND SPACE ADMINISTRATION
Goddard Space Flight Center
Greenbelt, Md.

Under
Contract NAS5-20994

by

Axel F. Brisken

General Electric Company
Corporate Research and Development
Schenectady, N.Y.

GENERAL ELECTRIC

SRD-77-038

ACKNOWLEDGMENTS

The author wishes to thank Richard L. Frey and James R. Lewis for Assembly and operation of the hardware necessary to provide the calibration data.

Page
Intentionally
Left Blank

Page
Intentionally
Left Blank

TABLE OF CONTENTS

LIST OF ILLUSTRATIONS

LIST OF ILLUSTRATIONS (Cont'd)

LIST OF TABLES

Section 1

INTRODUCTION

The successful implementation of future land mobile, maritime, aeronautical and satellite surveillance ranging and position fixing via geostationary satellites depends on the system's ability to conduct accurate, precise and efficient range measurements. The key system component remains the active transponder aboard the vehicle. The purpose of the effort described within this report is the demonstration of remote L-band tone-code transponder ranging accuracy, precision and reliability.

The Applications Technology Satellites (ATS) of NASA have been used by General Electric since 1968 to test the concept of position location by range measurements from pairs of satellites to measure the factors that affect position fixing accuracy including the propagation delays in the ionosphere and to test the reliability of voice and digital communications between ground terminals and mobile craft. The work during the first two phases[1] of NASA Contract NAS5-11634 was restricted to the use of the VHF transponders on ATS-1 and ATS-3.

Work at L-band using the ATS-5 satellite began with Phase 3[2] of NASA Contract NAS5-11634. In 1971 an automatic tone-code ranging transponder was designed, constructed and used to compare ranging measurements and communications reliability at VHF and L-band and to measure the performance of the tone-code technique at L-band. A contribution to practical implementation of L-band was made by the development of a solid-state RF power amplifier and receiver. The transponder was equipped for voice communications through the VHF satellite. Voice transmissions, like the tone-code signals, employ narrow bandwidth frequency modulation.

Results of the ranging experiments confirmed that ranging resolutions measured in hundreds of meters at VHF and tens of meters at L-band could be achieved within the ratio frequency bandwidths used for communications with simple, inexpensive, automatic equipment. The ranging signals can be compatible with communications and the range measurements can be accomplished in a time that is negligibly short compared to the signal durations used for communications.

Experiments conducted by the General Electric Company and Exxon Corporation from mid-1973 to early 1974[3] with the tanker ESSO BAHAMAS demonstrated near

real-time position fixing of NASA's ATS-1 and ATS-3 satellites via a VHF network with remote transponders in Europe, Iceland, North and South America and Australia. These computed satellite positions were then used immediately to locate the ship.

Under NASA Contract NAS5-20034, L-band/VHF transponders were deployed near Honolulu, Hawaii and in Buenos Aires, Argentina to provide near real-time locations of ATS-5 and short term position predictions.[4,5] These transponders contained self-calibration circuits which removed variations in the analog circuit internal time delay as a significant source of range measurement error. Over a 24-hour period, L-band trilateration positions disagreed with NASA C-band range and range rate positions by less than 0.0002 degree in latitude and longitude and 20 m in earth center distance. Satellite position errors of this magnitude would contribute approximately 40 m line-of-position errors to a remote vehicle at 45 degrees from the subsatellite point. Direct comparisons with NASA positions suggested variations in the transponder internal time delays by as much as 0.7 μs.

Land mobile/satellite communications and position fixing experiments[6] conducted during mid-1976 at VHF through ATS-1 and ATS-3 demonstrated vehicle position fixing accuracy on the order of a hundred meters. Near simultaneous range measurements to a ground truth reference transponder in the vicinity of vehicle operations provided a real-time measure of the ionospheric propagation time delay. At large distances from the ground truth reference (several hundred kilometers), accurate vehicle positions depend on the homogeneity of the ionosphere.

The L-band transponder selected for the calibration exercises described within this report was that previously deployed in Hawaii.[4] The transponder operates on the tone-code ranging technique; 9.7656 kHz audio frequency tones modulate the carriers ± 20 kHz in a 60 kHz RF bandwidth. The correlator in the transponder matches the phase of the locally generated tone with that received from the master ground station via satellite (or directly in the laboratory). Phase matching is accomplished over 256 tone cycles, requiring less than 30 ms for phase matching and correlation. After correlation, the transponder generates a tone-code sequence similar to the interrogating signal for transmission to the master ground station.

The L-band transponder was recalibrated in the laboratory; local oscillators and mixers simulated the satellite and short pieces of cable, the satellite-ground station slant range. Under various controlled conditions, ranging interrogations of the

transponder demonstrated variations in transponder internal time delay due to transponder received RF carrier signal level, frequency offsets of the responder 10 MHz timing oscillator, temperature variations and frequency offsets of the received RF carrier.

Variations in the RF carrier signal level to the transponder were shown to affect changes of up to 0.25 μs in internal time delay. The fixed signal level of the self-calibration response cannot match the variable received level from the satellite and thus, cannot result in an accurate internal time delay correction. Similarly, variations in the received RF carrier frequency caused delay variations of several microseconds; the fixed frequency of the self-calibration response cannot track the received frequency. Variations in the frequency of the transponder receiver or transmitter, however, would be correctable by the self-calibration technique. Control by the master ground station could accommodate drifts in the satellite frequency translation oscillator and doppler shift and thus, reduce error contributions from this mechanism.

The self-calibration circuits have previously been shown to correct for temperature induced delay variations in the responder tuned circuits. The calibration exercises verified a full corrective capability.

The responder 10 MHz timing oscillator had been suspected of generating delay variations during transponder deployment in Hawaii. Similar delay variations were deduced for the L-band transponder in Buenos Aires. The calibration exercises verified a linear dependence between the transponder internal time delay and the frequency of the timing oscillator; variations of one part in 10^6 would change the transponder internal time delay through 0.53 μs. As the transponder self-calibration circuits measure only the analog circuit phase delay, they are incapable of reporting a drift in the timing oscillator. Oscillators stable to within one part in 10^8 would generate maximum one meter satellite-transponder slant range errors.

Of the 111 calibration exercises, 28 were conducted under nominal (yet controlled) conditions. The transponder internal time delay remained stable over a two month period and the average delay over all measurements agreed with that theorized for the transponder. Residual variations on the order of tens of nanoseconds caused random variations in the individual mean time delays. These variations are speculated to result from variations on the order of several hundred Hertz in the frequencies of the transponder and master ground station transmitters.

The transponder stability demonstrated during these calibration exercises exceeded that previously achieved by more than an order of magnitude. The next level of calibrations must include measurements of the master ground station and transponder receiver and transmitter frequencies, to within tens of Hertz.

Section 2

OBJECTIVES

The objectives of the effort described within this report were to identify and quantify factors which affect the performance of the L-band tone-code-data ranging transponders developed under NASA Contract NAS5-11634 and deployed and operated under NASA Contract NAS5-20034. Specific objectives include the following tasks:

- Assemble at the General Electric Radio-Optical Observatory the L-band ranging transponder previously deployed in Hawaii for the tracking of the ATS-5 satellite (NASA Contract NAS5-20034).
- Configure the Observatory to conduct calibration exercises with the L-band transponder.
- Conduct sufficient calibration experiments to demonstrate factors which degrade transponder accuracy, precision and reliability, to quantify these factors where possible and to verify long term transponder stability under controlled conditions.

Section 3

EQUIPMENT DESCRIPTION

3.1 TONE-CODE RANGING TECHNIQUE

Ranging measurements to satellites are made by measuring the two-way radio propagation time of a signal between a ground station and the satellite. Following corrections for the propagation time delay of the ionosphere and troposphere and the internal time delays in the satellite and ground station, the ranging time can be converted to a slant range by relating it to the known speed of light. Propagation time is measured by placing a time marker in the form of a tone-code interrogation (Figure 1) on the transmitted signal and observing its two-way transit time. As used in this experiment, the interrogation signal consisted of a short audio frequency tone followed by a digital synchronization and address code in which an audio tone cycle was inhibited for a digital "0" and transmitted for a digital "1."

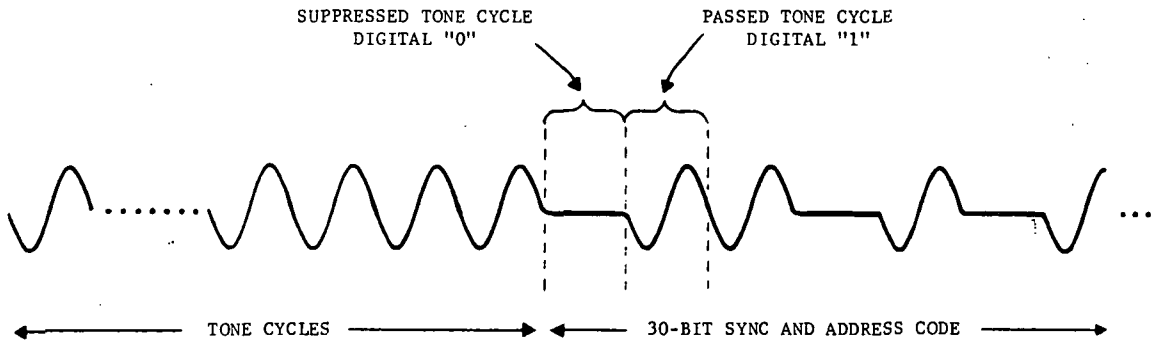

FIGURE 1. TONE-CODE RANGING WAVEFORM

A master ground station can determine the slant range from itself to the satellite by the above mentioned technique. The slant range from the satellite to any number of other remote ground stations can be determined if the ground stations are equipped to acknowledge a tone-code interrogation and transmit a tone-code response after a precisely defined time delay. The other ground stations may be fully automatic transponders.

A unique digital address code identifies each remote transponder. When the satellite-transponder slant range is to be determined, the ground station transmits a tone burst followed by the transponder address code. The satellite repeats the tone-

code interrogation and all remote transponders within the satellite line-of-sight receive the retransmission. Only the transponder which recognizes its address code will transmit a tone-code response. The satellite repeats the transponder's response; automatic muting prevents the transponder from acknowledging reception upon the second repetition of its address code by the satellite. The master ground station recognizes the address code as the one it sent and records the master ground station-satellite two-way ranging time and the master ground station-satellite-transponder two-way ranging time. To obtain measurements of the slant ranges from the satellite to several transponders, the master ground station interrogates them in sequence.

Figure 2 depicts the basic tone-code transponder configuration. When a transponder receives tone cycles from the satellite, they are applied to the phase matching circuit even though they may be part of an interrogation for another transponder. The phase matcher adjusts the phase of the locally generated tone of the same frequency such that it corresponds to the phase of the received tone. Averaging

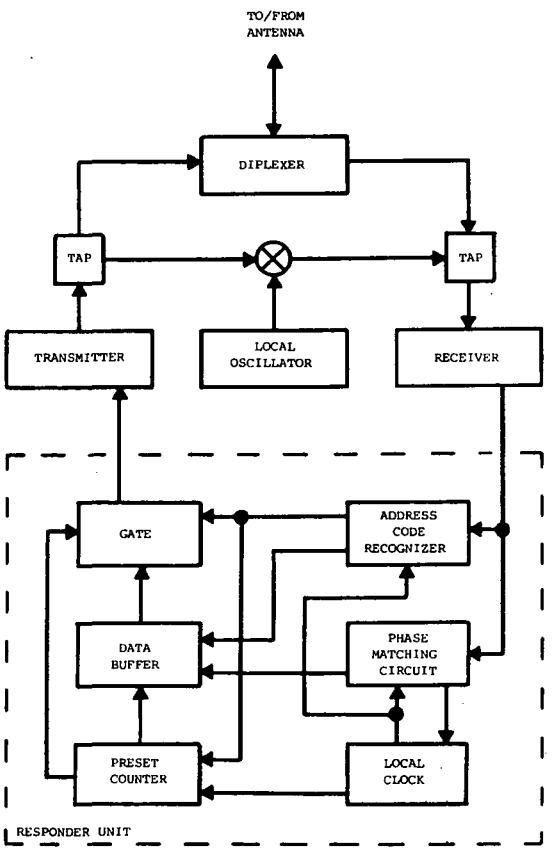

FIGURE 2. BASIC TONE-CODE TRANSPONDER CONFIGURATION

over many cycles improves phase matching accuracy (by the square root of the number of cycles).

The phase-matched, locally generated tone clocks the received interrogation signal into an address code recognizer, a shift register with summing circuits prewired to correspond to the unique digital address code of the transponder. When the sequence of pulses representing the transponder address code is loaded into the recognizer and acknowledged by the transponder, the recognition circuit produces a single, unambiguous output pulse which simultaneously keys the transmitter and starts a counter which measures out a precise number of locally generated tone cycles. Clock pulses reapplied to the shift register cause the address code to be clocked out to the transmitter following a preset number of tone cycles. In this way the transponder transmits its unique address code after a precisely defined time delay following correlation.

At the master ground station, the receiver output is applied to an address code recognizer similar to that in the transponder. Prior to the interrogation of a particular transponder, the taps of the summing circuit are switched to correspond to the transponder address code. When the address code is received from a satellite, a single output clock pulse occurs at the output of the summing circuit.

The L-band transponder contains a self-calibration circuit to measure the equipment internal time delay on every range measurement. Variations in the transponder and Observatory time delays occur primarily in the analog and RF circuit to and from the responder logic sections. Typical daily temperature variations can cause the internal time delay to vary through approximately 5 μs, which if uncorrected, would generate slant range measurement errors of 750 m.

As sketched in Figure 2, the transponder contains reactive signal samplers (TAP's) which remove a small fraction of the transponder's response transmission from the output of the power amplifier. A double-balanced mixer and local oscillator translate this sample through the same frequency difference as the satellite converts the uplink frequency to the downlink frequency. A second reactive signal sampler injects the self-calibration looped signal (appearing identical to satellite downlink) into the transponder receiver. The receiver demodulates the mixed transmitted signal and passes the audio tone to the responder. The total L-band signal delay from the output of the responder back through its input varies from one unit to another; typical values are slightly greater than one complete audio tone cycle.

After a preset period of time sufficient to allow the self-calibration signal to settle in the tuned circuits of the responder, the phase of the received tone is compared (over 256 cycles) with the phase of the tone being transmitted; the resulting phase difference is loaded into a data buffer. Following the complete transmission of the tone-code response, the responder sends a digital data stream to the master ground station. Digital data include the number of received address code bits in error at correlation and a representation of self-calibration signal phase difference. To improve transmission reliability, three tone cycles represent a digital "1" while three suppressed tone cycles represent a digital "0." At the master ground station, the phase difference may pass directly to a computer for ranging time correction and slant range calculation.

Ideally, the self-calibration loops should include all components through which the ranging signals pass. Practically, however, components such as the diplexer, transmit and receive cables and antenna feed elements are excluded as their delays can be measured independently and are not expected to vary beyond the accuracy limits of the range measurements.

3.2 TRANSPONDER CONFIGURATION

The L-band transponder shown in the block diagram of Figure 2 was designed for fixed frequency operation. Signals were received from the satellite at 1550.455 MHz and transmitted at 1651.475 MHz. The fixed antenna on the spinning ATS-5 satellite has a 50 ms window every 780 ms, thus setting the requirement for short duration ranging tones and transponder interval time delays of approximately 530 ms.

Detailed discussions of the L-band transponder receiver, exciter, power amplifier, self-calibration loop (at RF), and diplexer have been previously presented.[4] The responder unit is the core of the tone-code ranging technique and a description of its operation follows.

The responder unit shown in the block diagram of Figure 3 is the digital logic center of the L-band transponder. It accepts audio frequency signals from the L-band receiver and operates in the following sequential manner:

- matches the phase of a locally generated tone with the phase of the received tone,
- recognizes its unique digital address code and subsequently generates a response,

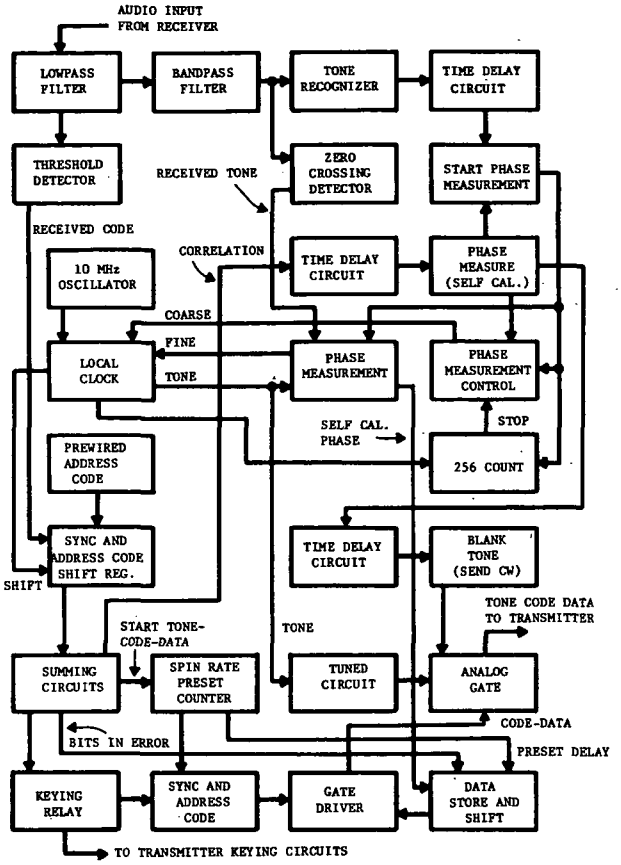

FIGURE 3. RESPONDER FUNCTIONAL DIAGRAM

- performs necessary timing functions to match the response delay with specified "windows," and
- digitizes the manual settings of the delay thumbwheel switches, the number of address code bits in error at correlation and the responder self-calibration response allowing them to be transmitted as digital data following the tone-code ranging response.

A detailed description of the operation of the responder has been previously provided.[7,8]

The audio output of the receiver passes through low pass and bandpass filters which reduce noise that may be present on the received signal. The audio frequency tone is applied to a zero crossing detector and to a tone recognition circuit. The zero crossing detector hard limits the signal accurately about its zero crossings, producing a square wave with precisely defined rise and fall times corresponding to the zero crossings of the input audio frequency tone. The tone recognition circuit consists of a

narrow bandwidth filter and switching circuit that produces a zero output under no-tone conditions and positive output when tone is present. Applying the output of the tone recognition circuit to a 20 to 30 ms time delay circuit insures that the phase measurement process does not start before the filters have arrived at a steady state.

When tone has been recognized and the time delay circuit has allowed sufficient time for the steady state phase to be reached, a start pulse stops the responder clock. A 10 MHz oscillator drives this clock which generates the local 9.7656 kHz. The clock is restarted on the next zero crossing of the received waveform, making a course adjustment in the setting of the clock such that the received and locally generated tone phases are within ± 5 μs. The received and locally generated tones are in the form of square waves from the zero crossing detector and the clock, respectively.

Fine phase matching continues through the next 256 audio tone cycles. Counters accumulate the phase difference between the rising and falling edges of each cycle of the received tone and locally generated tone. A final adjustment in the setting of the responder clock is based on the mean phase difference over 256 cycles. Averaging over 256 cycles instead of relying on a single comparison reduces the phase matching error due to phase jitter on the received tone by a factor of 16.

Following completion of phase matching, the receiver output signal is passed through a lowpass filter, on to a threshold detector for code and to a 30-bit synchronization and address code shift register. In the event that the received address code matches that prewired into the responder, correlation occurs and control circuits initiate a ranging response. As the output of the threshold detectors is hard limited, the random nature of noise may sometimes generate a sequence of 1's and 0's that correspond to the unique digital address code of the responder. Correlation would thus occur prematurely. Noise may also precipitate the exchange of 1's and 0's in the received address code. Correlation may only occur in an adjustable 10 to 30 ms code "window" which is opened immediately following fine phase matching. Correlation may occur with up to four bits in error in the 30-bit synchronization and address code sequence.

A preset counter with three octal (0-7) thumbwheel switches controls the number of tone cycles sent to the L-band transmitter before the responder sends the synchronization word and address code, thus providing for passage of the ranging response through any specified "window," such as the "window" of the spinning ATS-5

satellite. The position of each switch is stored as a digital number in a data buffer. The prewired minimum number of tone cycles is 3956, corresponding to 405094.4 μs. Adjusting the thumbwheel switches can increase this delay in increments of 409.6 μs.

Upon correlation, the responder counts down from the preset counter while generating the 9.7656 kHz audio frequency tone in phase with the received tone. When the appropriate counter has reached 174, the 15-bit synchronization word and 15-bit digital address code are transmitted. When the counter has reached 144, data is transmitted; when the counter has reached 0, the ranging response has been completed and transmission ceases.

During tone transmission, reactive signal samplers on the L-band transmit cables remove a small fraction of the RF power. A mixer translates the RF signal through 101.020 MHz, the translation frequency of the satellite. The resultant transponder self-calibration signals are injected into the appropriate receive cables by the same type of reactive signal samplers.

The self-calibration phase measurement sequence starts exactly 135 ms after correlation. The phase measurement gate is reopened, starting the 256 tone cycle counter and clearing the phase measurement register. Over 256 cycles, the average of the time differences between the received and transmitted rising edge and between the received and transmitted falling edge is divided by 256 and accumulated in the phase measurement register. A decreasing count in the phase measurement register from 4096 (0000) to "n" indicates that the received tone phase lags the transmitted tone phase by 4096-n tenths of microseconds. A typical response of 370.0 μs indicates a phase difference of 39.6 μs.

The number of received address code bits in error during correlation, the settings of the manually adjustable thumbwheels specifying the responder time delay and the self-calibration phase measurement are saved as digital numbers in a data buffer. The response ranging tone is applied through a lowpass filter converting the digital square waveform to an analog sinusoidal waveform for frequency modulation on the appropriate carriers. When the address code is to be transmitted, the sequence of 30 binary numbers is shifted synchronously with the audio tone cycles to suppress one audio cycle for a "0" and to transmit one audio cycle for a "1." Forty-eight bits representing the stored data are clocked into the gating circuit at one-third the clock rate to suppress three consecutive audio tone cycles for a digital "0" and to allow the

transmission of three consecutive tone cycles for a digital "1." The lower rate insures a low bit error rate on the received data.

Following completion of the tone-code-data transmission, the responder is muted for 0.35 second to prevent the tone recognition circuits from initiating a response on the satellite return of the transponder's response. At the end of the muting period, the responder is ready for the next interrogation.

The self-calibration circuit does not measure the absolute signal delay through the transponder, only the phase difference. The approximate absolute delay is determined by calibration measurements. The self-calibration circuit will not correct for delay variations due to responder 10 MHz timing oscillator frequency offset; it provides only a measure of the phase delay through the analog circuits to and from the responder logic sections.

3.3 CALIBRATION EQUIPMENT CONFIGURATION

The equipment configuration used at the General Electric Radio-Optical Observatory in the laboratory calibration of the L-band transponder is shown in Figure 4.

The automatic address code sequencher determines the order or remote transponder interrogation and whether the interrogation is to be transmitted at L-band or at VHF.

All timing and synchronization circuits, clocks and time interval counters at the Observatory are referenced to a Manson RD180 frequency standard with a stability better than 5 parts in 10^{10}.

The synchronizer triggers range measurement interrogations on second ticks of the Observatory time-of-day clock. On command from the synchronizer, the tone-code generator sends approximately 768 cycles of audio tone followed by the 15-bit synchronization word and the 15-bit digital address code. The interrogation drives the Observatory exciter for a tone-code transmission. When the last complete cycle of address code has left the tone-code generator, the generator starts the second and third time interval counters to measure the Observatory-transponder-Observatory ranging time and the Observatory self-calibration time.

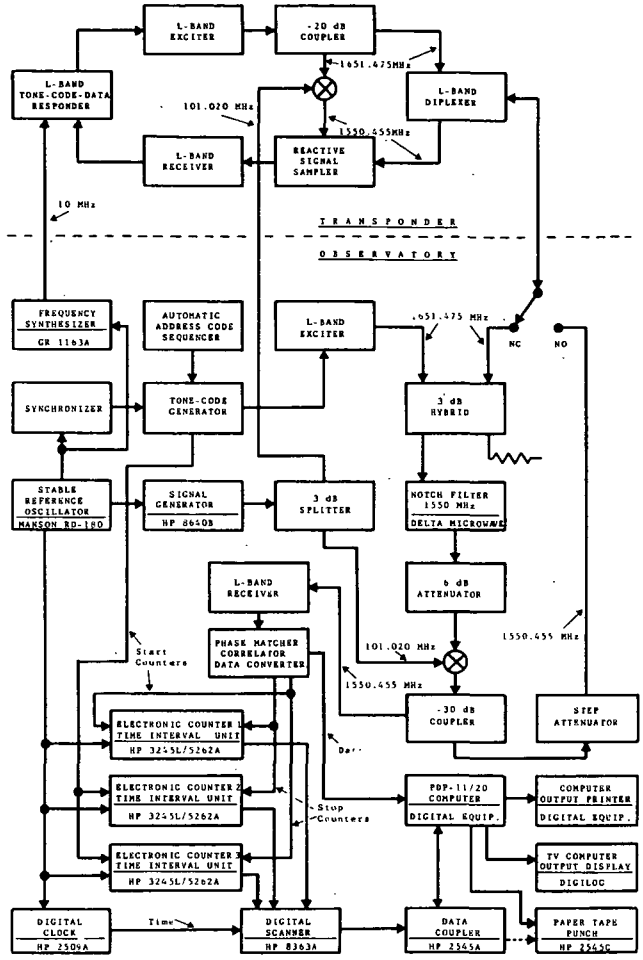

FIGURE 4. TRANSPONDER CALIBRATION EQUIPMENT CONFIGURATION

L-band transmissions from the Observatory exciter (previously discussed[4]) pass to a double-balanced mixer for conversion to the receive frequency. A -30 dB coupler samples part of the translated transmission and passes it to the Observatory receiver for a measurement of the Observatory internal time delay. The translated transmission is also sent to the transponder under test via the transmit/receive relay (normally in the receive position). Upon transponder correlation, the same initial mixer converts the transmit frequency to the receive frequency and the response is passed to the Observatory in a manner identical to the passage of the Observatory self-calibration signal.

Figure 5 presents a block diagram of the Observatory receiver, built in modular form from discrete components. It closely resembles the receiver system used during L-band trilateration exercises.[4]

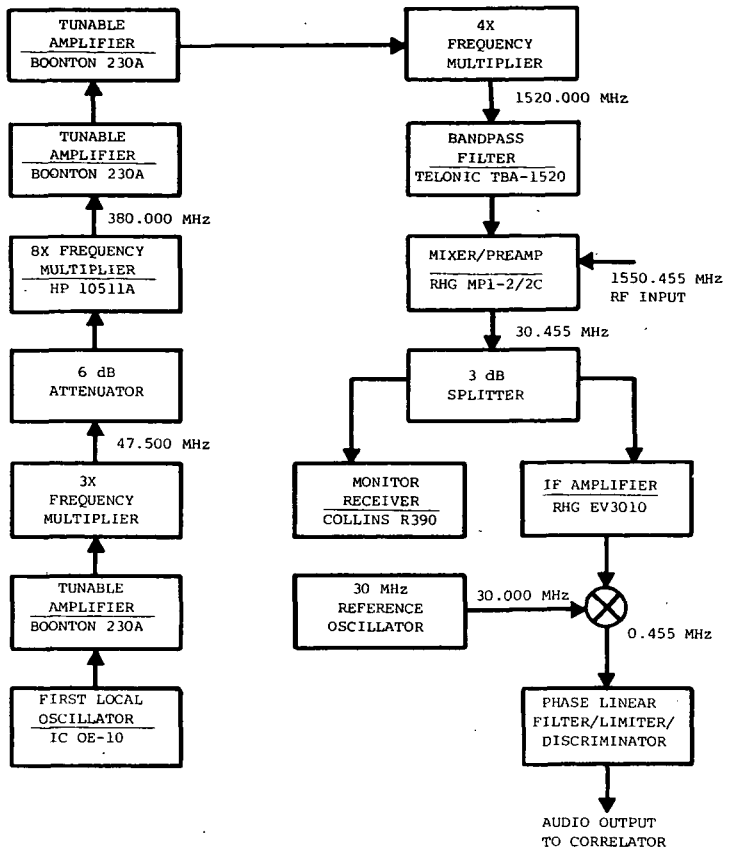

FIGURE 5. BLOCK DIAGRAM OF OBSERVATORY L-BAND RECEIVER

The first Observatory phase-match/correlation process (self-calibration; Observatory internal time delay) starts before the complete tone-code interrogation has left the exciter. On correlation, the third time interval counter is stopped yielding a measure of the Observatory internal time delay. The first time interval counter is also started at this time. The second Observatory phase-match/correlation process (ranging time to transponder) occurs on the transponder response, approximately one-half second after completion of the interrogation. On Observatory correlation, the first and second time interval counters are stopped for measurements of the ranging time to the transponder, with and without the Observatory internal time delay. The Observatory correlator is wired to show a ranging time to the transponder of approximately 639 ms if the transponder failed to correlate and 630 ms if the Observatory detected the response tone but could not correlate.

The Observatory correlator circuits function in a manner similar to the correlator of the remote transponder. At fine phase matching, the remote transponder correlator rounds off the adjustment of its local clock phase to the nearest 0.1 μs. The

Observatory, however, truncates the measured phase difference at the 0.1 μs digit but also transmits to the computer the most significant bits of the phase comparison thus allowing range measurement resolutions to 0.0004 μs. This resolution applies to ranging times to the transponder and to the Observatory internal time delay.

A separate circuit in the Observatory correlator decodes the data stream following the address code in the responses from the remote transponders. This digital data stream contains the setting of the adjustable responder thumbwheel switches which define the transponder "logic" time delay, the number of bits in error during transponder correlation and a digital respresentation of the transponder self-calibration response.

The outputs of the three time interval counters and the output of a digital clock pass automatically through a digital scanner and a data coupler to a high speed paper tape punch or to the PDP-11/20 digital computer. Adjustment of thumbwheel switches on the digital scanner causes the appropriate month, day, year and file number identifying each experiment to be punched on paper tape or entered into the computer following each line of ranging data. In addition, the PDP-11/20 computer receives digital data from the correlator relating the most significant bits of the Observatory phase comparison the setting of the responder internal time delay thumbwheel switches, the number of bits in error during transponder correlation and the response of the transponder self-calibration circuits.

The punched paper tape and computer output formats are shown in Figure 6. Data identification numbers are alternately printed several times near the beginning of each data file. All tapes are punched in ASCII code. The first column of eight digit numbers contains the ranging time to the remote transponder (third column of eight digit numbers) less the Observatory internal time delay (fourth column of eight digit numbers). The second column of eight digit numbers contains the transponder address code (11) and the time of day in hours, minutes and seconds. The fifth column of four digit numbers contains the response of the transponder self-calibration circuit. The last two columns of three digit numbers contain the fine phase measurement residual on the ranging time to the transponder and on the Observatory internal time delay.

3.4 TRANSPONDER INTERNAL TIME DELAY

The ranging time T_r to a transponder under calibration by the technique shown in Figure 4 may be expressed as

```
01092351 11174337 06389760 03297408 0000 000 000 000
01047989
05297533 11174339 05298946 00001412 3715 000 143 160
01047989
05297533 11174341 05298947 00001413 3716 000 130 029
01047989
05297533 11174343 05298946 00001412 3716 000 025 071
05297532 11174345 05298945 00001412 3716 000 124 013
05297531 11174347 05298943 00001411 3715 000 077 199
05297532 11174349 05298946 00001413 3716 000 211 068
05297534 11174351 05298947 00001412 3717 000 249 206
05297534 11174353 05298948 00001413 3716 000 226 222
05297531 11174355 05298945 00001413 3717 000 239 016
05297532 11174357 05298945 00001412 3716 000 174 220
05297530 11174359 05298944 00001413 3717 000 110 032
05297530 11174401 05298944 00001413 3717 000 152 192
05297535 11174403 05298948 00001412 3716 000 139 188
05297533 11174405 05298947 00001413 3716 000 154 006
05297531 11174407 05298943 00001411 3716 000 153 232
05297533 11174409 05298947 00001413 3716 000 017 177
05297533 11174411 05298946 00001412 3716 000 205 200
05297532 11174413 05298945 00001412 3716 000 077 231
05297532 11174415 05298946 00001413 3716 000 038 047
05297532 11174417 05298945 00001412 3717 000 204 183
05297535 11174419 05298948 00001412 3715 000 236 192
```

FIGURE 6. TYPICAL COMPUTER PRINTOUT OF TRANSPONDER CALIBRATION DATA

$$T_r = \delta_{to} + \delta_{ci} + \delta_r + \delta_{cr} + \delta_{ro} , \tag{3.1}$$

where

δ_{to} = internal time delay between the Observatory interrogator and the output of the Observatory transmitter,

δ_{ci} = cable propagation time from the Observatory transmitter to the transponder receiver (0.0403 μs for the circuit of Figure 4),

δ_r = internal time delay of the transponder between the input of the receiver and the output of the transmitter,

δ_{cr} = cable propagation time from the transponder transmitter to the Observatory receiver (0.0866 μs for the circuit of Figure 4) and

δ_{ro} = internal time delay between the Observatory receiver and the Observatory correlator.

A measurement of the Observatory internal time delay is made on every interrogation of the transponder. The measured value of this delay T_o includes the cables between the output of the transmitter and the input of the receiver, and is given by

$$T_o = \delta_{to} + \delta_{co} + \delta_{ro} , \tag{3.2}$$

where

δ_{co} = cable propagation delay (0.0635 μs for the circuit of Figure 4)

and where all other symbols remain as previously defined.

The transponder self-calibration circuit measures the phase difference between the transmitted audio frequency tone and that received via the self-calibration loop. This comparison takes place in the logic sections of the transponder. The transponder analog circuit internal time delay δ_a is thus the sum of an integer number n of audio tone cycles of period δ_i (102.4 μs) plus the measured phase difference. The measured phase difference is represented as 409.6 μs less the response of the self-calibration circuit δ_{sc}; the transponder analog circuit internal time delay thus becomes

$$\delta_a = n\,\delta_i + 409.6 - \delta_{sc} - \delta_{cs} , \tag{3.3}$$

where

δ_{cs} = cable propagation time from the transponder transmitter to the transponder receiver (0.0134 μs for the circuit of Figure 4).

Following correlation, the remote transponder counts out a precise number of audio tone cycles m (3956) plus a variable number of cycles specified by the setting of transponder thumbwheel switches. The total transponder internal time delay δ_r (from the receiver input to the transmitter output) may be written as

$$\delta_r = m\,\delta_i + 409.6\,(S_3 + 8S_2 + 64S_1) + \delta_a + \varepsilon , \tag{3.4}$$

where

S_1,S_2,S_3 = setting of the manually adjusted transponder internal time delay thumbwheel switches (4,6,0 for the work described in this report) and

ε = residual unspecified components of the transponder internal time delay.

Combining Equations 3.3 and 3.4, the transponder internal time delay becomes

$$\delta_r = n\,\delta_i - \delta_{sc} + \varepsilon + 530022.3866, \tag{3.5}$$

where all units are microseconds.

Combining Equations 3.1 and 3.2, the measured value for the transponder internal time delay becomes

$$\delta_r = T_r - T_o - 0.0634. \tag{3.6}$$

Substituting Equation 3.5 and defining a macroscopic internal time delay d_r as

$$d_r = T_r - T_o + \delta_{sc}\ , \tag{3.7}$$

the residual internal time delay ε becomes

$$\varepsilon = d_r - n\delta_i - 530022.4500. \tag{3.8}$$

The macroscopic internal time delay comprises only those quantities which are measured on every ranging interrogation; the macroscopic internal time delay is equal to the true transponder internal time delay less a constant representing primarily cable delays.

Previous calibration exercises have yielded a value of unity for n such that

$$\varepsilon = d_r - 530124.8500. \tag{3.9}$$

The primary function of the calibration exercises thus becomes the measurement of a near zero value for ε and the consequent verification of Equation 3.5 as the correct model for the definition of the transponder internal time delay. These measurements

should be conducted under a variety of circumstances to demonstrate transponder time delay stability or variation under non-ideal conditions.

3.5 RANGE MEASUREMENT PRECISION

Of the several factors affecting the precision achievable with the tone-code ranging technique, the most severe is that due to noise accompanying the ranging tone. A theoretical analysis of this effect as reported by Milton[9] shows that for a frequency modulated carrier, the lower limit on the range measurement standard deviation is given by

$$\sigma_{RF} = \frac{1}{2\pi \Delta F} \left[T(C/N) \right]^{-1/2} \tag{3.10}$$

where

ΔF = peak frequency deviation

T = ranging tone duration,

C/N = carrier-to-noise density at IF.

The above equation assumes ideal demodulation of the signal. A modulation index of approximately 2 yields a value of 20 kHz for ΔF, given a modulating tone frequency of 9.7656 kHz. The 256 cycles of the ranging tone used to phase match the clock of the responder result in an effective tone duration of 26.2 ms. The theoretical ranging resolutions presented in Table 1 consider several values of carrier signal-to-noise ratio.

The transponder correlator rounds off the time of arrival of the tone burst to the nearest 0.1 μs, yielding a maximum error of ± 0.05 μs. Assuming that round off errors from -0.05 to +0.05 μs are equally probable, the transponder correlator generated ranging time standard deviation σ_{TC} becomes 0.029 μs. The Observatory correlator truncates the ranging time at the 0.1 μs digit. Assuming that ranging time errors from 0.0 to 0.1 μs are equally probable, the Observatory correlator generated ranging time standard deviation remains the same with a 0.05 μs bias error. The Observatory correlator, however, also passes the most significant digits of the phase comparison (to a resolution of 0.0004 μs) to the computer allowing significant improvement in the measurement of the tone phase time-of-arrival. Use of the phase comparison digits reduces the Observatory correlator generated ranging time standard deviation to a negligible amount and eliminates the bias error.

Table 1

THEORETICAL RANGING RESOLUTION AT L-BAND DUE TO RF NOISE

Carrier Signal-to-Noise (dB)	C/N in 60 kHz Bandwidth (dBHz)	σ_{RF} (μs)
4.8	52.6	0.115
6.0	53.8	0.100
10.0	57.8	0.063
15.0	62.8	0.036
20.0	67.8	0.020

As the Observatory transponder RF propagation path remains fixed, no contributions to ranging time standard deviation result from the recording of the time at which the interrogation left the Observatory hardware or from the transmittal of the ranging response a finite time later. Satellite motion would vary the RF propagation path, affecting both the accuracy and precision of range measurements.

During the phase comparison process, the correlators accumulate pulses of the 10 MHz timing oscillator between the rising edges of the received and clock audio tone and between the falling edges of the same. For every zero crossing (256 rising, 256 falling), the pulse counter may accumulate errors from -0.05 to +0.15 μs. With noisy signals, these errors are equally probable and yield a pulse truncation standard deviation of 0.058 μs and a bias error of +0.05 μs. Over 512 zero crossings (256 audio tone cycles), the mean pulse counter standard deviation δ_{PC} reduces to 0.003 μs, with a bias error of +0.05 μs; the measured phase difference will be 0.05 μs greater than the true phase difference. This standard deviation and bias error must be added to the correlator generated standard deviation and bias error (if any).

For received audio tones with no noise, pulse counter errors from -0.05 to +0.15 μs are not equal probably resulting in a mean error between -0.05 and +0.15 μs over 256 tone cycles. If a +0.05 μs bias is assumed, error bounds on the phase-matching of ±0.1 μs must be considered. These error bounds are not a standard deviation.

A signal with a 0.05 μs standard deviation on each zero crossing is defined as the boundary between clean and noisy signals. Zero crossings of signals of this quality

will have a 9.4 percent probability of being outside of the -0.05 to +0.15 μs range of probable errors; a 31 percent probability of being ±0.05 μs beyond the bias. By Equation 3.10, a signal with a 0.05 μs standard deviation in one-half wavelength (51.2 μs) will have a 19.4 dB carrier-to-noise ratio. Random errors in the measurement of the tone time-of-arrival due to errors in the pulse counter at each rising and falling edge will begin to appear above this carrier-to-noise ratio. A signal with a ±0.005 μs standard deviation (39.4 dB C/N) would have a 5×10^{-9} percent probability of being outside the −0.05 to +0.15 μs range of probable errors and a 97 percent probability of being within a 0.03 μs wide interval on every zero crossing. Non random phase-matching errors of up to 0.07 μs will result. The L-band transponders and the Observatory were not designed to operate with signal strengths of this magnitude.

Section 4

CALIBRATION EXERCISES AND RESULTS

Factors which change the effective transponder internal time delay include propagation path degradations of the ranging interrogation and response and local instabilities within the transponder itself. Ionospheric scintillation, variations in the spacecraft effective isotropic radiated power to the transponder, the movement of the satellite within the narrow beamwidth of a transponder antenna and variations in the satellite-transponder distance will combine to generate changes in the transponder received signal strength from the satellite. Similar variations plus changes in transponder transmit power would also affect the satellite-master ground station propagation path on the ranging response. Subsection 4.1 discusses variations in the effective transponder internal time delay as a function of the received signal strength at the transponder and at the master ground station.

Doppler shifts due to satellite motion, drifts in the satellite frequency translation oscillator and variations in the transponder RF local oscillators will combine to change the frequency of the signal received by the remote transponder. These factors do not significantly affect, however, the modulation on the carrier. The master ground station need not suffer from variations in the received RF carrier frequency since personnel will be available to retune receivers as necessary. Subsection 4.2 discusses variations in the effective transponder internal time delay as a function of received RF frequency.

Local temperature changes may vary the performance characteristics of components within the transponder receiver, responder analog input and output circuits and transponder transmitter, resulting in a variation of the transponder internal time delay. The transponder self-calibration circuit measures the phase delay of the ranging tone through these components on every ranging interrogation. Phase measurements are transmitted to the master ground station in the tone-code-data ranging response. Subsection 4.3 discusses the corrective ability of the self-calibration circuits.

Following correlation, the responder generates a precise number of audio tone cycles before transmitting the response synchronization and address codes. Variations in the frequency of the audio tone will vary the effective transponder internal time delay. Subsection 4.4 discusses the dependence of the internal time delay on the

frequency of the responder 10 MHz timing oscillator, the local reference standard for the generation of the audio frequency tones.

Subsection 4.5 discusses the effective transponder internal time delay with the perturbing factors of above fixed at nominal values. This summary includes the results of several tests over a two-month period.

4.1 INTERNAL TIME DELAY VS. RECEIVED SIGNAL STRENGTH

During the previous calibration of the L-band transponders,[4] no tests for internal time delay variation with respect to received signal strength had been conducted. Signal strength variations have been observed[6] degrading ranging precision and causing changes of up to one microsecond in the transponder internal time delay per 10 dB of change in carrier-to-noise ratio.

A series of 15 tests demonstrated the dependence of L-band transponder time delay accuracy, precision and reliability as a function of the received signal strength. During these tests, the Observatory receive signal levels for the Observatory self-calibration and the transponder response were kept at a constant 15 dB carrier-plus-noise-to-noise ratio; for the transponder self-calibration loop, the same. The step attenuator of Figure 4 varied the signal level from the Observatory to the transponder. In operational configurations, transponder self-calibration signal levels would be set at deployment to a level representative of the satellite downlink. Therefore, variations in downlink signal level could not be corrected by variations in the fixed self-calibration signal level.

Figure 7 depicts the transponder macroscopic internal time delay (see Subsection 3.4, Equation 3.7) as a function of transponder received carrier-to-noise ratio. The internal time delay is seen to decrease through approximately 0.22 μs from just above the FM detection threshold to a C/N of 20 dB. Most of the change occurs within 6 dB above the detection threshold. The single data point identified with the "X" represents an increase in the transponder self-calibration signal to a C/N of 17.5 dB with a nominal interrogation C/N of 15 dB. The error bars on Figure 7 reflect one sigma standard deviations of the mean. Individual data points represent mean values of 35 to 129 separate measurements; most data points represent approximately 90 individual measurements.

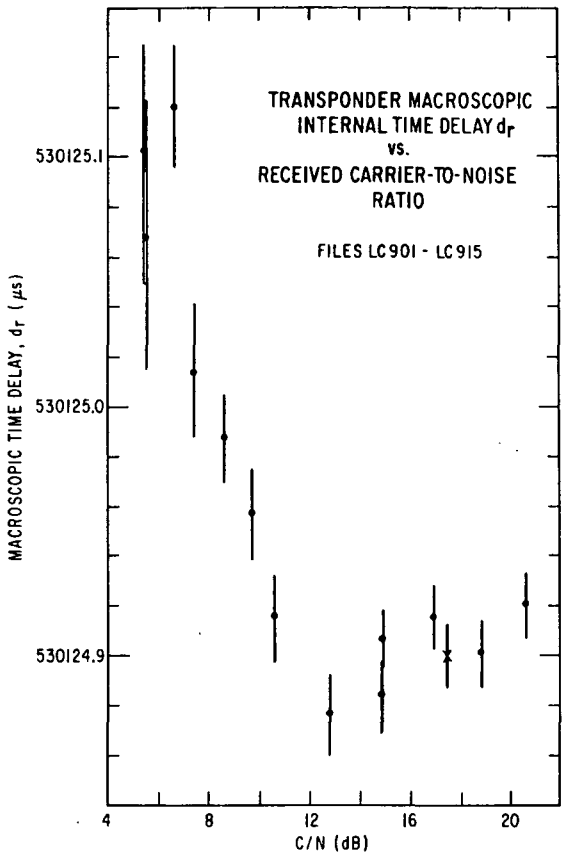

FIGURE 7. TRANSPONDER MACROSCOPIC INTERNAL TIME DELAY AS A FUNCTION OF RECEIVED CARRIER-TO-NOISE RATIO

All macroscopic internal time delay computations (Equation 3.7) for the data of Figure 7 reflect usage of the fine-phase measurement bits on the Observatory-transponder ranging time and the Observatory internal time delay measurements (see Subsection 3.3). Neglecting these data results in no change in delay values since the expression for macroscopic internal time delay requires the difference in the two Observatory measurements; delay errors of 0.05 μs cancel each other. Unless otherwise specified, all further results presented in this report reflect the fine-phase data bits on Observatory measurements.

Standard deviations of individual macroscopic internal time delay measurements as a function of received signal level are shown in Figure 8, with the dots and X's reflecting nonconsideration and consideration of the Observatory fine-phase measurement data, respectively. The two lines reflect absolute minimum theoretical standard deviations (maximum precisions), the top solid curve with the fine-phase data and the bottom dashed curve without these data. Table 2 itemizes the individual factors which

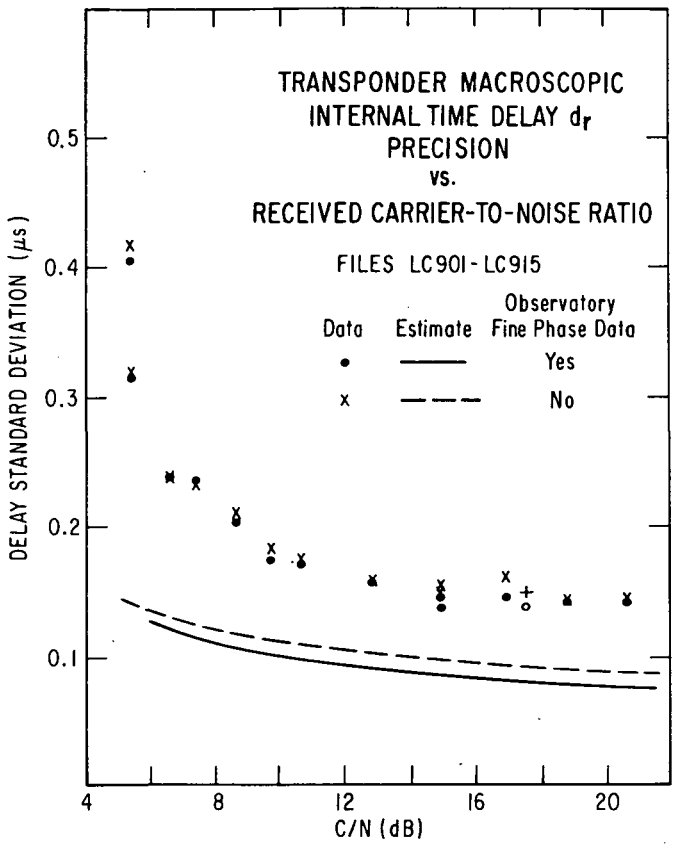

FIGURE 8. PRECISION OF TRANSPONDER MACROSCOPIC INTERNAL TIME DELAY MEASUREMENT AS A FUNCTION OF RECEIVED CARRIER-TO-NOISE RATIO

contribute to the theoretical estimates of precision. While the experimental results show a greater standard deviation than estimated, they do verify improved precision with the use of the Observatory fine-phase measurement data. The large disagreement between observed and theoretical precision at low carrier-to-noise ratios results from the nonconsideration of threshold effects in Equation 3.10. An explanation for the remaining disagreement is beyond the scope of this report.

The single data points represented by the open circle and the "+" reflect an increased signal level on the transponder self-calibration instead of the ranging interrogation, as previously discussed.

As seen from the data of Figure 9, the transponder can be expected to correlate on virtually all ranging interrogations with carrier-to-noise ratios in excess of approximately 7 dB. FM detection threshold effects reduce and eventually completely prevent correlation for signals below this level.

Table 2

CONTRIBUTIONS TO MACROSCOPIC INTERNAL TIME DELAY;
ONE SIGMA STANDARD DEVIATION

Measurement Component	Source of Standard Deviation	Without Observatory Fine-Phase Data (μs)	With Observatory Fine-Phase Data (μs)
Observatory-transponder ranging time, T_r	Transponder FM demodulation, σ_{RF}	Eq. 3.10	Eq. 3.10
	Transponder correlator roundoff, σ_{TC}	0.029	0.029
	Transponder correlator pulse counter, σ_{TP}	0.003	0.003
	Observatory FM demodulation, σ_{RF}	0.036	0.036
	Observatory correlator roundoff, σ_{OC}	0.029	0.000
	Observatory correlator pulse counter, σ_{OP}	0.003	0.003
Observatory internal time delay, T_o	Observatory FM demodulation, σ_{RF}	0.036	0.036
	Observatory correlator roundoff, σ_{OC}	0.029	0.000
	Observatory correlator pulse counter, σ_{OP}	0.003	0.003
Transponder self-calibration, δ_{sc}	Transponder FM demodulation, σ_{RF}	0.036	0.036
	Transponder correlator roundoff, σ_{TC}	0.029	0.029
	Transponder correlator pulse counter, σ_{TP}	0.003	0.003
Root sum square (less contribution for σ_{RF} from Eq. 3.10)		0.085	0.075

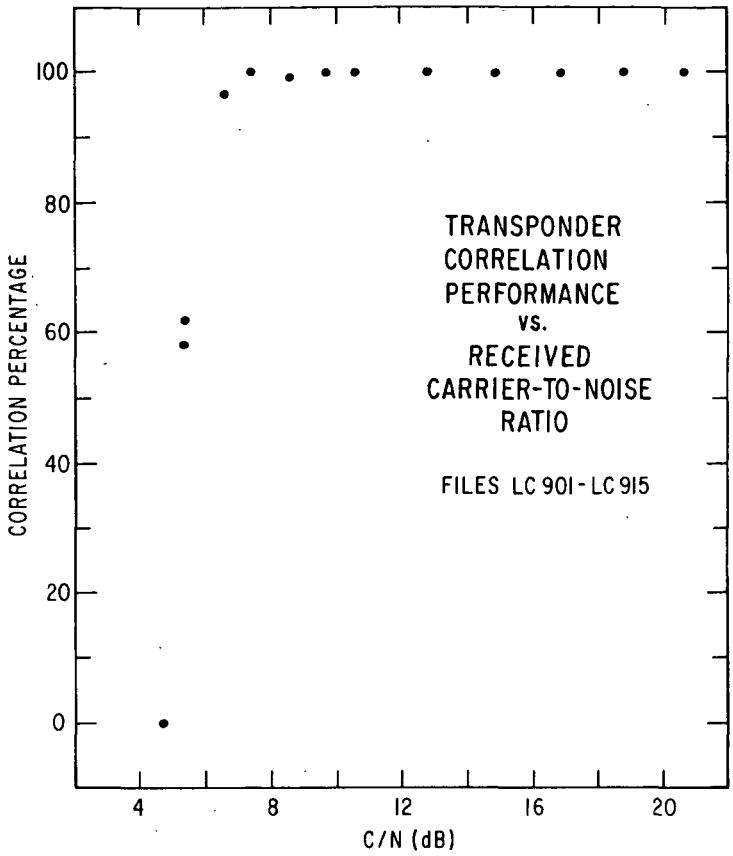

FIGURE 9. PERCENTAGE OF TRANSPONDER CORRELATION TO RANGING INTERROGATIONS AS A FUNCTION OF RECEIVED CARRIER-TO-NOISE RATIO

In a similar set of tests, the Observatory self-calibration and the transponder response signal levels were changed while the transponder self-calibration and interrogation stayed fixed at a nominal carrier-to-noise ratio of 15 dB. Contrary to the case of a deployed remote transponder, the Observatory self-calibration signal level can be changed at any time to match that on the satellite downlink. The self-calibration circuit should thus completely correct for any received signal strength variations. As the downlink signal levels on the satellite return of the Observatory interrogation and transponder response may differ, the Observatory self-calibration signal level may have to be switched between the two levels to allow for a full correction.

The data of Figure 10 show slight, yet significant variations in the effective transponder internal time delay due to the failure of the Observatory self-calibration circuit to fully correct for the variation in received signal strength. From the FM detection threshold to a carrier-to-noise ratio of approximately 8 dB, the internal time delay increases by 0.1 μs; above 8 db, the time delay remains constant.

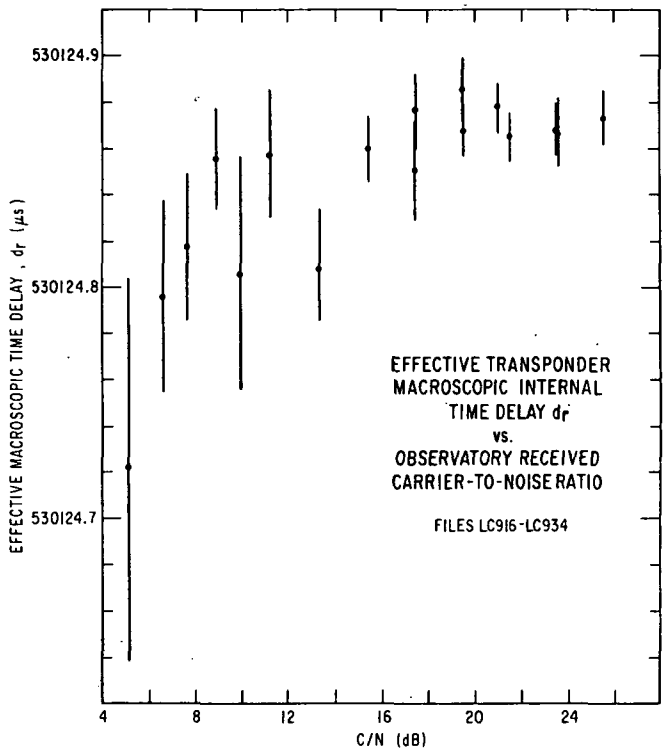

FIGURE 10. TRANSPONDER MACROSCOPIC INTERNAL TIME DELAY AS A FUNCTION OF OBSERVATORY RECEIVED CARRIER-TO-NOISE RATIO

The dots of Figure 11 show one sigma standard deviations of individual macroscopic internal time delay measurements as a function of received signal strength at the Observatory. The measurements and theoretical estimate of absolute minimum standard deviation (solid curve) reflect usage of the Observatory fine-phase measurement data. Similar to the results of Figure 8, the observed standard deviation exceeds that predicted, particularly for low carrier-to-noise ratios where FM detection threshold effects dominate.

Figure 12 depicts Observatory correlation on the transponder response as a function of the Observatory received carrier-to-noise ratio and shows correlation on virtually all responses for signal levels above 6 dB (C/N). Below carrier-to-noise ratios of 6 dB, FM detection threshold effects become prominent and eventually prevent correlation due to the lack of demodulated signals. During tests at low signal levels, the Observatory failed to correlate on approximately the same number of self-calibration measurements as transponder responses. Both quantities are equally vital for an accurate value of transponder internal time delay, or operationally, satellite-transponder slant range.

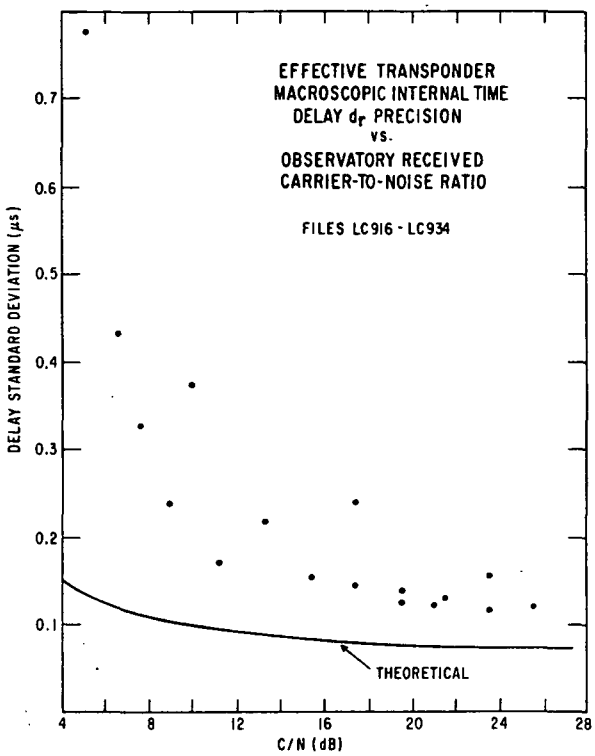

FIGURE 11. PRECISION OF TRANSPONDER MACROSCOPIC INTERNAL TIME DELAY MEASUREMENT AS A FUNCTION OF OBSERVATORY RECEIVED CARRIER-TO-NOISE RATIO

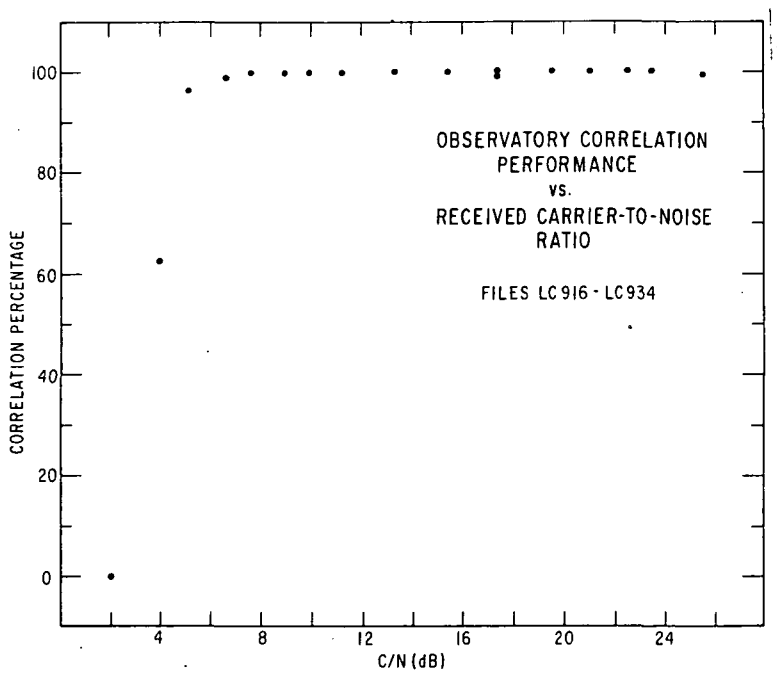

FIGURE 12. PERCENTAGE OF OBSERVATORY CORRELATION TO TRANSPONDER RANGING RESPONSES AS A FUNCTION OF OBSERVATORY RECEIVED CARRIER-TO-NOISE RATIO

4.2 INTERNAL TIME DELAY VS. RECEIVED RF CARRIER FREQUENCY

In an operational environment, the Observatory and transponder transmit and receive frequencies and the satellite translation frequency may drift, resulting in off frequency reception of ranging signals. The Observatory and transponder exciters contain RF crystal oscillators with stabilities of two parts in 10^6 over a -30 to +60 ^oC temperature range. In a laboratory environment, temperature variations in excess of 20 Centigrade degrees are rare. Prior to the calibration exercises described in this report, both exciters were set to the same center frequency. Throughout the tests, the exciters remained within several hundred Hertz of each other, approximately one part in 10^7.

The Observatory L-band receiver relies on the oscillator within the Collins R390 monitor receiver (see Figure 5) for the selection of the proper receive frequency. The frequency of the 15.833 MHz oscillator is adjusted to zero beat the 30.455 MHz in the R390. Following warmup, the R390 will maintain frequency to within approximately 200 Hz, approximately one part in 10^7.

The transponder receiver first local oscillator at 1520.000 MHz uses a temperature compensated crystal with a stability of one part in 10^6 over a 0 to +60 ^oC temperature range. The second local oscillator (crystal controlled) operates at 30.000 MHz with a rated stability of one part in 10^5. In a laboratory environment, the transponder receiver may be expected to maintain frequency to within several hundred Hertz. The transponder receiver was put onto center frequency prior to the calibration experiments.

As shown in Figure 4, frequency stability for the self-calibration frequency translation/satellite simulator oscillators was provided by the Observatory frequency standard.

To demonstrate the magnitude of the effective remote transponder time delay variation as a function of received frequency, the frequency synthesizer for the transponder self-calibration loop was fixed at the satellite translation frequency. A second, identical frequency synthesizer supplied the Observatory self-calibration/satellite translation frequency in 2 kHz steps on both sides of the satellite translation frequency. The Observatory receiver was retuned for each test so that only the transponder received ranging signals off center frequency, and only from the Observatory; the transponder self-calibration signals remained nominal. Figure 13 depicts the effective transponder macroscopic internal time delay as a function of frequency offset

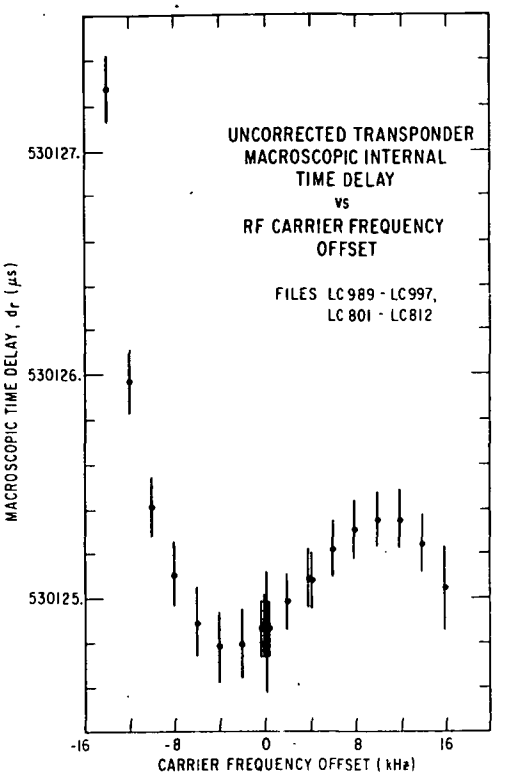

FIGURE 13. UNCORRECTED TRANSPONDER MACROSCOPIC INTERNAL TIME DELAY AS A FUNCTION OF RECEIVED RF CARRIER FREQUENCY OFFSET (The transponder self-calibration signal was maintained on nominal center frequency.)

on the received ranging interrogation. The delay variation is not symmetric about center frequency, most probably due to improperly aligned sections of the transponder receiver 0.455 MHz filter. The macroscopic time delay at center frequency is consistent with that observed during several other tests. In the vicinity of center frequency, the internal time delay changes at a rate of approximately 6.0×10^{-5} μs/Hz.

Operation of the transponder self-calibration oscillator at the same offset frequencies will allow the self-calibration circuit to measure the receiver delay due to off frequency received signals and thus, provide for a correction of the ranging time. Figure 14 shows that the self-calibration corrected macroscopic internal time delay remains stable for offset RF carriers from -5 to +15 kHz. The inability to correct at offset frequencies from -15 to -5 kHz results from the steep delay variation slope on the left side of Figure 13. An average delay rate of change of approximately 2.2×10^{-4} μs/Hz (at an offset of -10 kHz) would require a difference between the Observatory and transponder transmit frequencies of 450 Hz; a drift of transmit frequency of this magnitude is well within the specifications on the transmitter

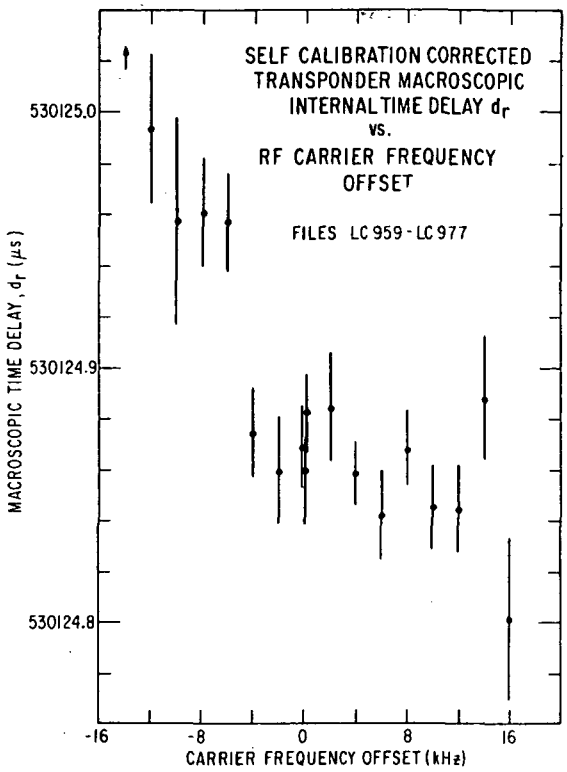

FIGURE 14. CORRECTED TRANSPONDER MACROSCOPIC INTERNAL TIME DELAY AS A FUNCTION OF RECEIVED RF CARRIER FREQUENCY OFFSET. (The transponder self-calibration carrier frequency was equal to the offset ranging interrogation carrier frequency.)

oscillators and consistent with the frequency differences noted during the tests. At center frequency, a transmitter frequency difference of 450 Hz would generate a 0.027 μs change in transponder internal time delay. The data presented in Figure 13 and 14 therefore appear consistent. The data points of Figures 13 and 14 each represent mean values of separate tests with 51 to 147 individual measurements per mean value.

Figure 15 depicts the one sigma standard deviations of individual macroscopic internal time delay determinations as a function of RF carrier frequency offset. The dots represent data taken with the self-calibration correction of internal time delay (both frequency translation oscillators shown in Figure 4 offset by the same amount); the X's, without the self-calibration correction. There appears to be no significant systematic variation of precision as a function of carrier frequency offset.

Transponder correlation performance is centered almost exactly around the nominal receive frequency of 1550.455 MHz, as shown in Figure 16. The dots and X's represent transponder correlation percentages with and without calibration correction

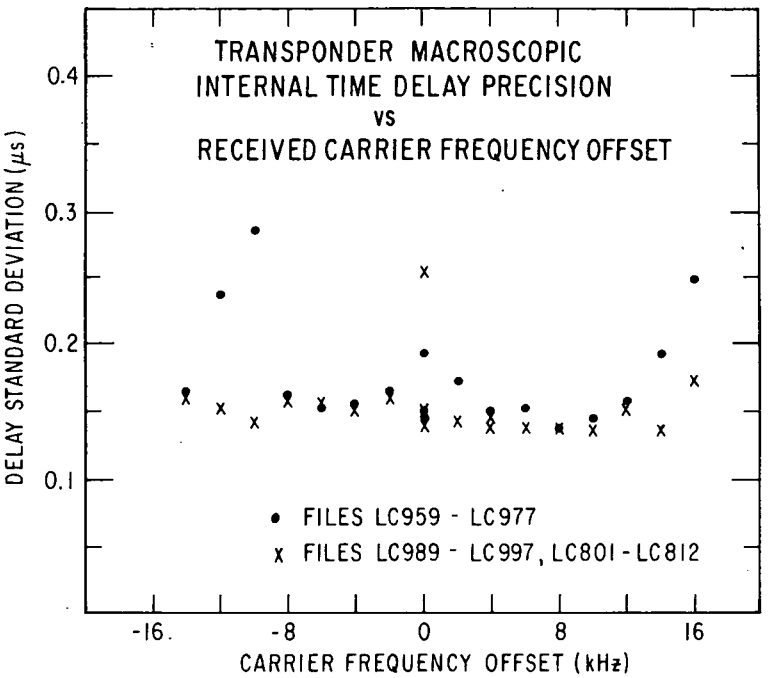

FIGURE 15. PRECISION OF TRANSPONDER MACROSCOPIC INTERNAL TIME DELAY MEASUREMENT AS A FUNCTION OF RECEIVED RF CARRIER FREQUENCY OFFSET

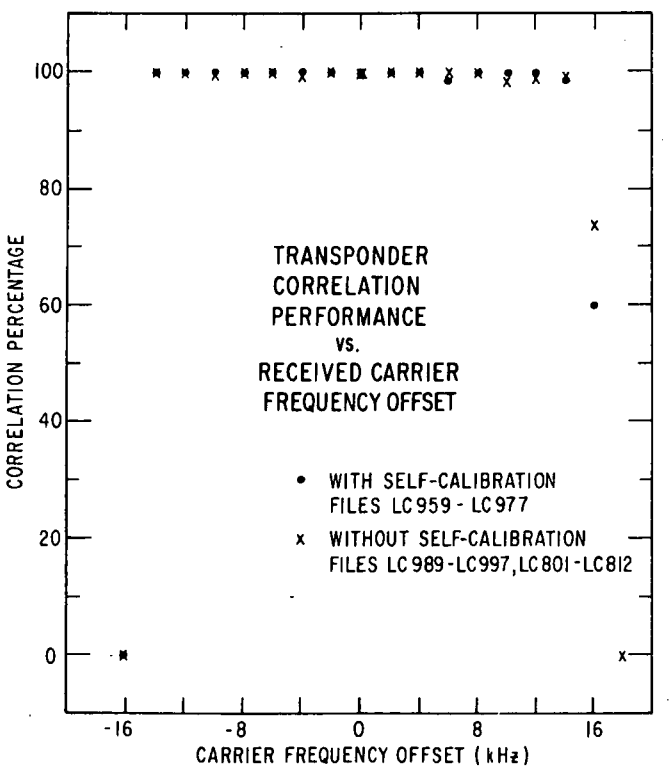

FIGURE 16. PERCENTAGE OF TRANSPONDER CORRELATION TO RANGING INTERROGATIONS AS A FUNCTION OF RECEIVED RF CARRIER FREQUENCY OFFSET

of the ranging time. The transponder will correlate on virtually all interrogations provided the receiver and RF carrier frequencies disagree by no more than 14 kHz. During the tests with self-calibration correction of the ranging time, the transponder correlated on all self-calibration signals, even at carrier frequency offsets (±16 kHz) where the correlation on the ranging interrogation become intermittent.

4.3 INTERNAL TIME DELAY VS. TRANSPONDER TEMPERATURE VARIATIONS

The data of Figure 17 demonstrate the stability of the transponder internal time delay against variations in temperature. The top set of data points of Figure 17 represent individual measurements of the Observatory-transponder ranging time. At a time of approximately 20:02:20 GMT, the responder tuned circuits were cooled by a spray of liquid freon, with a resultant increase in the ranging time due to an increase in the transponder internal time delay. The bottom set of data points reflect the corresponding responses of the self-calibration circuit and show a decreasing value due to cooling. The sum of the ranging time and the self-calibration response less the Observatory internal time delay was defined in Subsection 3.4 as the macroscopic transponder internal time delay, the middle set of data points on Figure 17. The macroscopic internal time delay differs from the true transponder internal time delay by only a constant. The data of Figure 17 show no variation in time delay due to cooling.

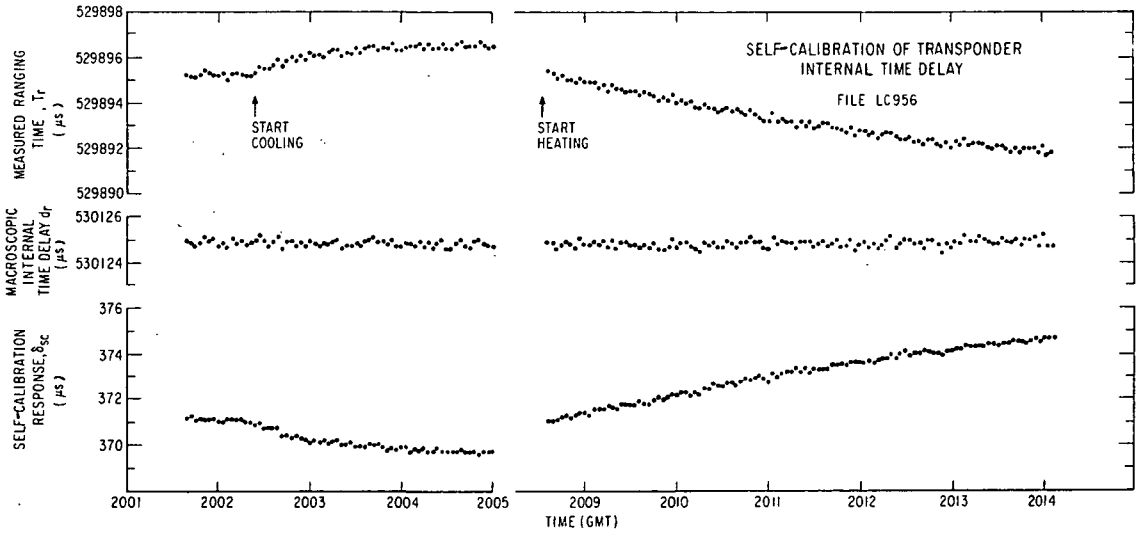

FIGURE 17. SELF-CALIBRATION CORRECTION OF MEASURED TRANSPONDER INTERNAL TIME DELAY

The three sets of data points on the right side of Figure 17 reflect ranging measurements while the responder tuned circuits were subjected to a hot air blast. Opposite to measurement variations during cooling, the ranging time decreases with increased heat while the self-calibration response increases; the macroscopic transponder internal time delay remains constant.

Throughout the entire cold/hot cycle, the mean macroscopic internal time delay over 455 data points was 530124.8336 ±0.0070 μs, where the standard deviation reflects the mean. Over the individual segment of ranging data for the cold environment as presented in Figure 17, the 68 data points yield a mean macroscopic delay of 530124.8203 ±0.0163 μs; for the hot environment, 111 data points with a mean of 530124.8322 ±0.0137 μs. The insignificant change in transponder time delay (0.012 μs) due to the cold and hot environment is observed to be well within the one sigma standard deviations.

4.4 INTERNAL TIME DELAY VS. TIMING OSCILLATOR STABILITY

During the calibration of the L-band transponder scheduled for deployment in Hawaii,[4] a variation of the transponder internal time delay as a function of the responder 10 MHz timing oscillator had been observed. Furthermore, variations in the internal time delays of both transponders (in Buenos Aires and Hawaii) had been inferred from sinusoidal errors in measured transponder-ATS-5 slant ranges. This sinusoidal variation was correlated with the air temperature in the rooms containing the transponders.

Following the phase matching process, the responder clock frequency (9.7656 kHz) is entirely dependent on the responder 10 MHz timing oscillator. Should the oscillator frequency be higher than nominal, the responder will generate audio tone cycles at a faster rate with a subsequent reduction in the internal time delay. The internal time delay error E may be estimated by the expression

$$E = (D_1 + \delta_{tc} - \delta_{oc}) \left(1 - \frac{f}{f_o}\right), \qquad (4.1)$$

where

D_1 = responder logic delay ($\delta_r - \delta_a$, see Equations 3.3 and 3.4),

δ_{tc} = time between the end of phase matching and correlation in the responder on the ranging interrogation,

δ_{oc} = time between the end of phase matching and correlation in the Observatory correlator on the transponder response,

f = instantaneous frequency of the responder timing oscillator, and

f_o = nominal frequency of the responder timing oscillator (10 MHz).

The self-calibration circuit will not provide a correction for a frequency error in the timing oscillator. This circuit measures the phase difference between the responder output audio frequency tone and the tone passed to the responder input via the responder transmitter, the self-calibration loop and the receiver. The total time delay from responder output to responder input is on the order of 140 μs as compared to approximately 530 ms for the total internal time delay to a ranging interrogation. The self-calibration phase measurement will reflect the drift in timing oscillator frequency but it will be indistinguishable from and negligible compared to variations in the analog circuit delays.

The remote transponders complete phase matching approximately 19 ms ($\delta_{tc} \approx 22$ ms) prior to the start of the ranging interrogation synchronization and address codes; at the Observatory, approximately 22 ms ($\delta_{oc} \approx 25$ ms) prior to the start of the response code sequence. With a total logic time delay of approximately 529.6 ms, Equation 4.1 becomes

$$E = 526.6 \left(1 - \frac{f}{f_o}\right) \text{ ms} . \qquad (4.2)$$

The experiment configuration of Figure 4 was used to determine the internal time delay variations as a function of timing oscillator frequency offset. (C+N)/N ratios for all RF signals into the Observatory and transponder receivers were set to approximately 15 dB. Throughout the calibrations described in this report, the Observatory's General Radio 1163-A frequency synthesizer passed 10 MHz to the responder; the normal 10 MHz crystal oscillator had been disabled. The synthesizer referenced the Observatory's Manson RD 180 frequency standard.

Figure 18 contains a composite representation of the variation of the macroscopic internal time delay d_r as a function of responder timing oscillator frequency offset. The solid dots represent varying delays for offsets from -20 to +20 Hz; the x's represent one tenth of the delays for frequency offsets ten times greater than listed on the abscissa ($\pm$200, $\pm$100, $\pm$50 Hz); the open circles represent the next

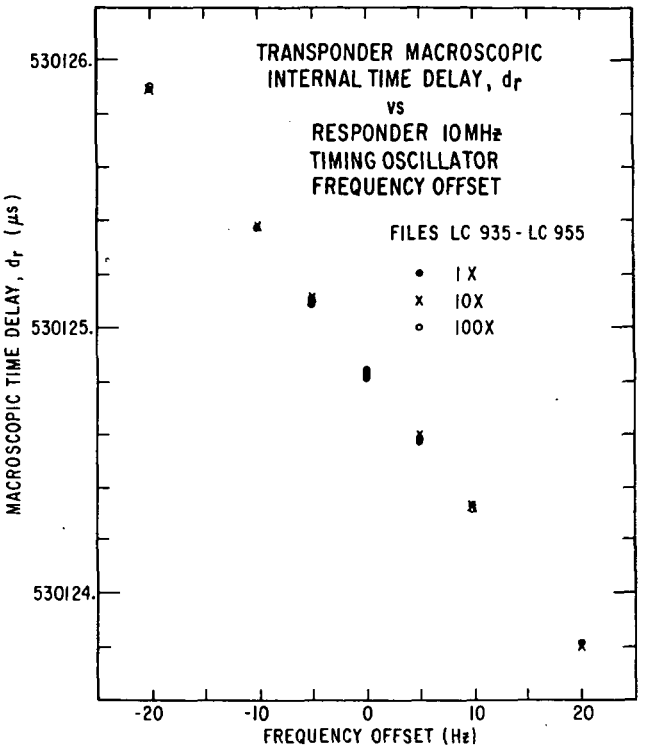

FIGURE 18. TRANSPONDER MACROSCOPIC INTERNAL TIME DELAY AS A FUNCTION OF RESPONDER 10 MHZ TIMING OSCILLATOR FREQUENCY OFFSET. (The x's represent variations in time delay and offset frequency scaled down by a factor of 10; the open circles, by a factor of 100.)

order of magnitude (-2000, ±1000, ±500 Hz). Over the entire range of offsets from -2000 to +1000 Hz, the delay variations remain a linear function of the frequency offset, at the rate of 0.05262 μs/Hz. This observation agrees to within 0.076 percent of that estimated by Equation 4.2. The mean value of the observed macroscopic internal time delays for zero offset and the macroscopic internal time delays corrected for the specified offset is 530124.849 μs, with an insignificant standard deviation.

There appeared to be no correlation between variations in the 10 MHz timing oscillator and variations in the standard deviation of individual ranging times. Most one sigma standard deviations of individual measurements varied between 0.13 and 0.17 μs, consistent with previous observations. Furthermore, the responder operated well throughout the variation in timing oscillator frequency. The maximum frequency offset of 2000 Hz (one part in 5000) did not result in correlation failures.

4.5 LONG TERM TRANSPONDER STABILITY

The previous sections discussed major perturbing factors to transponder internal time delay stability. Throughout the 111 individual tests from November 16, 1976 to January 4, 1977 (identified by file numbers LC901 to LC997 and LC801 to LC812), 28 found the transponder in operation under nominal conditions (receive signal carrier-to-noise ratios of 15 dB, satellite frequency translation/self-calibration oscillators on center frequency, receive/transmit RF carrier frequencies within several hundred Hertz of center frequency, responder 10 MHz timing oscillator on center frequency). Throughout the tests, receive signal levels were measured with a true RMS voltmeter; the frequency translation/self-calibration and responder timing oscillators referenced the Observatory frequency standard; the transmit frequencies were observed by zero beating with the reference oscillator in the Observatory R390 monitor receiver; the receive frequencies were assumed within specifications.

Table 3 summarizes the controlled, nominal condition calibration exercises, giving the file number, date, time of day, number of individual measurements comprising the mean, the mean transponder macroscopic internal time delay and the one sigma standard deviation of the mean. The average transponder internal time delay over the 4177 individual measurements is 530124.847 $\pm$ 0.002 μs. Figure 19 is a plot of the internal time delay, arbitrarily given as a function of the time of day; Figure 20 depicts the one sigma standard deviation of individual measurements from the means of Table 3 and Figure 19, also shown as a function of time of day.

The mean transponder internal time delays of Figure 19 clearly do not follow a normal distribution; the data are corrupted by random perturbations. Mean values for 1400 individual measurements (33.5 percent) fall within one sigma standard deviations of the mean; for 2958 measurements (70.8 percent), within two standard deviations. The random perturbing factor is assumed to be the frequency difference between the Observatory and transponder exciters. The data of Figure 14 demonstrate self-calibration correction of transponder internal time delay due to receiver frequency offset; the same corrective capability is assumed for the Observatory internal time delay measurement. The data of Figure 14 further suggest a transmitter frequency difference of 450 Hz (not inconsistent with zero beating observations and consistent with other tests). At nominal RF carrier frequencies, 450 Hz would generate a 0.030 μs effective transponder internal time delay error for the transponder; the corresponding error for the Observatory has not been measured. A random error with maximum excursions of $\pm$0.030 μs would readily explain the non-Gaussian nature of the data of

Table 3

SUMMARY OF TRANSPONDER
INTERNAL TIME DELAY MEASUREMENTS

File	Date	Time (GMT)	Number of Measurements	Macroscopic Internal Time Delay (μs)
901	11/16/76	1620	104	530124.907 ± 0.013
905		1652	94	.884 ± 0.015
925	11/18/76	1928	107	.860 ± 0.015
935		2053	108	.839 ± 0.013
944	11/19/76	1505	252	.823 ± 0.012
945		1826	82	.838 ± 0.015
955		1946	102	.805 ± 0.016
956		2013	455	.834 ± 0.017
957	11/22/76	1513	234	.893 ± 0.012
957C		1546	395	.823 ± 0.008
959		2126	74	.860 ± 0.023
968		2205	80	.883 ± 0.016
977		2239	80	.869 ± 0.016
978	11/23/76	1509	135	.805 ± 0.016
979		1540	291	.866 ± 0.008
980	11/28/76	1552	132	.821 ± 0.014
981		1600	127	.805 ± 0.020
982		1628	161	.847 ± 0.011
983	11/29/76	1622	75	.887 ± 0.017
984		1635	241	.855 ± 0.011
985		1814	99	.863 ± 0.014
986		1842	119	.837 ± 0.014
987		2015	124	.836 ± 0.019
988		2135	102	.832 ± 0.015
989	1/4/77	1745	104	.863 ± 0.014
997		1850	104	.887 ± 0.015
801		1855	79	.839 ± 0.028
812		1952	117	.869 ± 0.014
Overall			4177	530124.847 ± 0.003

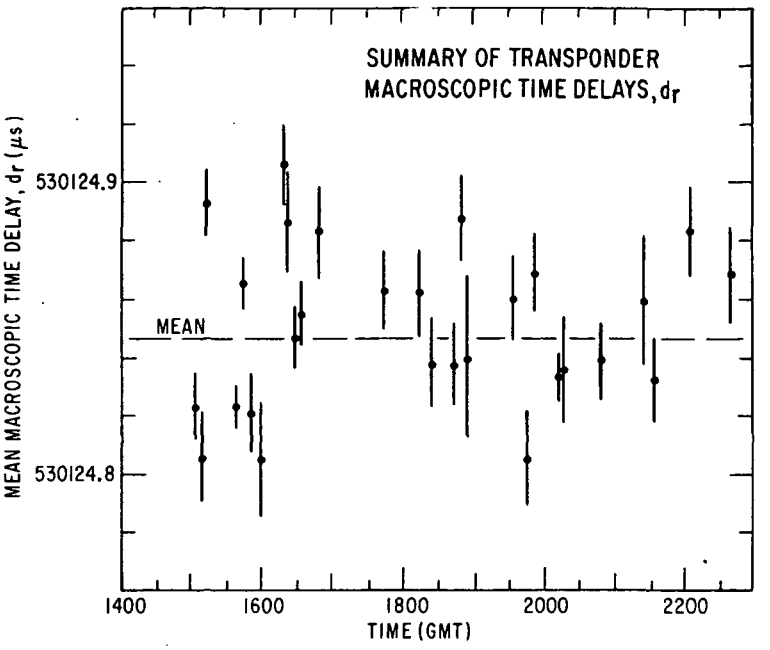

FIGURE 19. OVERALL TRANSPONDER MACROSCOPIC INTERNAL TIME DELAY AS A FUNCTION OF TIME OF DAY (These data represent calibration exercises under nominal, controlled conditions.)

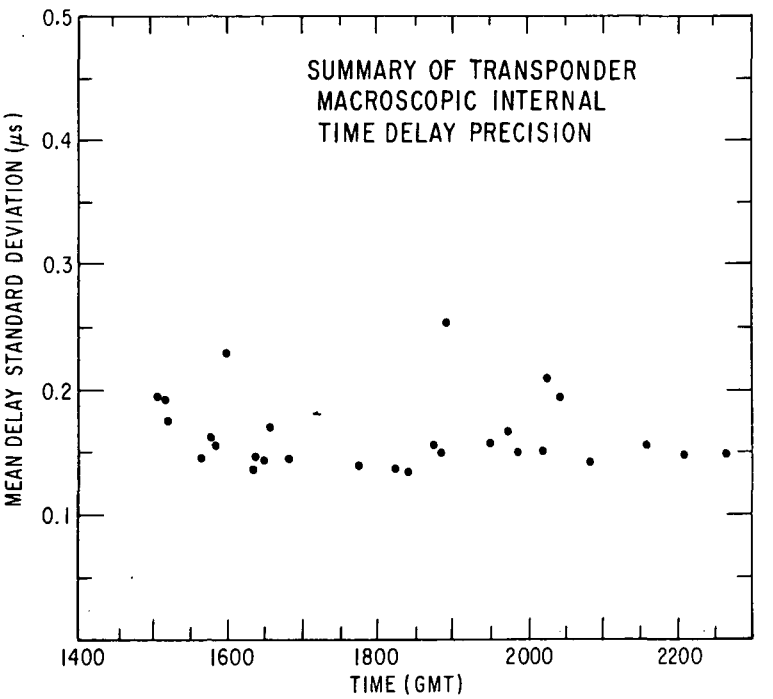

FIGURE 20. PRECISION OF TRANSPONDER MACROSCOPIC INTERNAL TIME DELAY MEASUREMENT AS A FUNCTION OF TIME OF DAY (These data represent calibration exercises under nominal, controlled conditions.)

Figure 19. The individual mean values disagree with the overall mean by less than +0.05 and -0.03 μs. Replotting the data of Figure 19 as a function of time of year did not reveal any systematic perturbation.

The one sigma standard deviations of individual transponder macroscopic, internal time delay measurements shown in Figure 20 do not show systematic variations. Averaged over the 4177 measurements of Figures 19 and 20, the individual measurement precision is 0.15 μs.

The overall macroscopic internal time delay of Table 3 shows excellent agreement with that theoretically estimated in Subsection 3.4, Equation 3.9 (530124.850 μs). The -0.003 μs value for the unspecified components of internal time equal to the standard deviation of the overall mean.

The only active component external to the self-calibration circuits during the transponder calibration exercises was the transponder diplexer. The diplexer contains two reject filters with notches 100 MHz removed from the center frequencies, a bandpass filter with a 3 dB bandwidth of 50 MHz and a broadband preamplifier (>100 MHz). Several previous attempts[4] to measure the propagation delay through the diplexer only verified the existence of greater perturbations (~0.020 μs) to transponder internal time delay stability. Due to its narrow bandwidth, the bandpass filter would have the greatest contribution to internal time delay. Assuming a maximum delay of 0.006 μs would change the value of ε to +0.003 μs, still within a one standard deviation of the mean. The lack of an exact diplexer internal time delay is not thought to seriously reduce confidence in the accuracy of the results as itemized in Table 3 and in the transponder delay model of Subsection 3.4.

Section 5

CONCLUSIONS

The purpose of this effort was the demonstration of long-term L-band tone-code ranging transponder internal time delay stability. This has been accomplished, along with a demonstration of factors that affect time delay accuracy.

Specific results of this effort with respect to transponder internal time delay accuracy are as follows:

- Under controlled conditions and over a two-month period, the average disagreement over 28 experiments (4177 individual measurements) between the theoretical and observed transponder internal time delay was 0.003 $\pm$ 0.003 μs. The model therefore accurately describes the transponder internal time delay.
- Under controlled conditions, transponder internal time delay mean values from individual tests over the two-month period disagreed with the overall mean by less than +0.05 and -0.03 μs; there remain no systematic variations.
- Between the FM detection threshold and RF carrier-to-noise ratios of 15 dB, the transponder internal time delay varies through 0.25 μs; between 15 and 22 dB, through 0.04 μs.
- Variations in the RF received carrier frequency of $\pm$ 2 kHz will contribute 0.1 μs internal time delay errors; the use of the self-calibration circuit allows corrections for carrier frequency offsets up to approximately $\pm$ 8 kHz.
- Temperature variations can change the transponder internal time delay by several microseconds; use of the self-calibration circuit totally eliminates temperature fluctuations as a source of effective time delay variation.
- Variations in the frequency of the 10 MHz responder timing oscillator will affect linear changes ($\sim$0.05 μs/Hz) in the transponder internal time delay; the self-calibration circuits will not correct for this error.
- Disagreements between the Observatory and transponder transmitter frequencies on the order of several hundred Hertz can generate effective internal time delay variations on the order of tens of nanoseconds after self-calibration time delay correction.

Specific results of this effort with respect to transponder time delay precision are as follows:

- Under controlled conditions, individual measurements of the transponder internal time delay had precisions of 0.15 μs.
- Between the FM detection threshold and RF carrier-to-noise ratios of 15 dB, the transponder time delay measurement precision improves from 0.4 μs to 0.15 μs; above 15 dB, the precision remains stable.
- The transponder time delay measurement standard deviation appears a factor of approximately two greater than predicted from a model which considers white noise in the demodulation process.
- The use of fine-phase measurement data (correlation resolution of 0.0004 μs) improves time delay measurement precision by approximately five to ten percent.
- Time delay measurement precision is unaffected by variations in the frequency of the received RF carrier.
- Variations in the frequency of the responder 10 MHz timing oscillator do not affect transponder internal time delay precision.

The transponder was found to correlate on virtually all ranging interrogations, with the following reservations:

- The FM detection threshold prevents transponder correlation for RF carrier-to-noise ratios below appfoximately 6 dB.
- Variations in the frequency of the received RF carrier through ±14 kHz will not prevent correlation; beyond ±14 kHz, the transponder will not correlate.
- Variations in the frequency of the responder 10 MHz timing oscillator do not prevent transponder correlation.

The calibration exercises verified the responder 10 MHz timing oscillator as a major factor in transponder internal time delay stability, as previously speculated.[4] The time delay stability demonstrated during this calibration exceeds that previously achieved by more than an order of magnitude.

Deployment of the L-band tone-code ranging transponder under controlled conditions will result in absolute transponder-satellite slant range errors of less than

several meters; individual slant ranges will have one sigma standard deviations of approximately 25 meters.

Future attempts to refine the transponder calibration technique must not only consider the factors demonstrated in Subsections 4.1 through 4.4, but must also consider the center frequencies of the Observatory and transponder receivers and transmitters. RF carrier stabilities limited the transponder stability to that quoted above.

Section 6

REFERENCES

1. Anderson, Roy E., "Final Report on Phases 1 and 2 - VHF Ranging and Position Fixing Experiment Using ATS Satellites," General Electric Company Report S-71-1109 under NASA Contract NAS5-11634, 1971.

2. Anderson, Roy E., "Final Report on Phase 3 - ATS Ranging and Position Fixing Experiment," General Electric Company Report SRD-73-062 under NASA Contract NAS5-11634, 1973.

3. LaRosa, Roy M., et.al., "Experimental Evaluation of Satellite Communications and Position Fixing for Maritime Users," Joint Final Report, Exxon Corporation and General Electric Company, June 1974.

4. Brisken, Axel F., "Final Report, ATS-5 Trilateration Support," General Electric Company Report for NASA Contract NAS5-20034, SRD-76-004, 1975.

5. Brisken, Axel F., "Location of ATS-5 by L-Band Trilateration," Navigation, Vol. 23, No. 2, pp. 106-118, Summer 1976.

6. Brisken, Axel F., Frey, Richard L., and Anderson, Roy E., "Application of Satellite Communication and Position Fixing Techniques to Land Mobile Systems," General Electric Company Report under Contract DEA-76-20, under preparation.

7. "Operation and Maintenance Manual, L-Band/VHF Transponder," General Electric Company Report, under preparation.

8. "Instructions and Operating Characteristics, Tone-Code Transponder System," General Electric Company Report, GEI-45099, April 1970.

9. Milton, Robert T., "Tone Code Ranging Precision," Memorandum, Ref. 2, 1971.